Archives of Computational Methods in Engineering (2021) 28:2409–2428
https://doi.org/10.1007/s11831-020-09460-y

ORIGINAL PAPER

A Review of Recent Trends and Challenges in Computational Modeling of Paper and Paperboard at Different Scales

Jaan-Willem Simon[1]

Received: 1 November 2019 / Accepted: 4 July 2020 / Published online: 25 July 2020

Abstract
Paper and paperboard are widely used in packaging products. The material behavior of paper and paperboard is very complex because different scales need to be considered in order to describe all relevant effects and phenomena. In particular, at least three scales can be distinguished: the fiber scale, network scale, and sheet scale. Since it is extremely challenging to measure the material behavior experimentally on all of these scales simultaneously, computational modeling of these materials has gained importance in recent years. This work aims at giving a systematic review of the numerical approaches and obtained results published in recent years. Focus is set on both the recent trends and achievements as well as challenges and open questions.

1 Introduction

There is a large potential for wood-fiber based materials such as paper and paperboard in numerous engineering applications. Classical applications of these materials are for example in the packaging of products such as food packaging, which is an important and still growing industry [196]. However, because of sustainability reasons in terms of renewability and recyclability, paper and board are also gaining importance in other applications as a substitute for e.g. building materials.

In order to optimize the design of both the materials and the products made of these materials, computational methods have been utilized more and more in the last decades. The major challenges to be coped with are the multi-physics and the multi-scale nature of paper. Even though the effects and phenomena occuring on the different scales are well-known and well described, see e.g. the general overview on paper physics provided in [4], it is still a field of ongoing research to account for them in numerical models.

There exist recent reviews that deal with specific aspects of the modeling strategies for paper and paperboard. In particular, in [77] recent applications of the finite element method (FEM) to paper, paperboard, and corrugated paperboards used in food packaging are summarized. However, focus is mostly on basic findings on the sheet level and structural scale whereas the multi-scale and multi-physics issues are not discussed. Another exhaustive review has been provided in [198] with the scope on forming processes of paper. There, three-dimensional deformations and damage mechanisms were recapitulated especially for deep-drawing, press-forming, hydro-forming, and others. These processes and the corresponding effects are comprehensively discussed. Nevertheless, also in this work the multi-scale character of the material is not addressed.

Thus, the aim of the current work is to sum up recent trends in the modeling of paper and board on the different scales of interest which are fiber, network, sheet, and laminate scales. In addition, the purpose of this systematic review is to discuss both achievements as well as drawbacks and open questions.

2 Modeling Paper on the Fiber Scale

On the fiber scale, the key aspects in modeling deal with the single fiber behavior and the bonds between individual fibers.

2.1 Single Fiber Behavior

While it is well-known that the single cellulose fibers consist of several different layers, in most approaches to model

✉ Jaan-Willem Simon
jaan.simon@rwth-aachen.de

[1] Institute of Applied Mechanics, RWTH Aachen University, Mies-van-der-Rohe-Str. 1, 52074 Aachen, Germany

their material response only the so-called S2-layer, which contributes most to the mechanical behavior, is considered. This layer is composed of a cellulose/hemicellulose/lignin matrix reinforced by microfibrils, see e.g. [52, 53].

The longitudinal material response in fiber direction strongly depends on the microfibril angle (MFA), which can vary significantly for different fibers [248]. Recent experimental methods to measure the mechanical behavior of fibers including their tensile strength are based on single fiber tensile tests, as shown in [159] for softwood and in [120] for hardwood fibers. In addition, the influence of humidity [121] and of refining as well as small-scale fiber deformations [132] on the single fiber strength have been investigated.

Even so, it is very challenging to measure the mechanical response of single fibers in the nonlinear regime. Thus, in most applications with consideration of the MFA, fibers are modelled linear elastic. Nevertheless, approaches to include the elasto-plastic behavior have been presented e.g. in [203], where the anisotropic yield criterion of Hill has been applied, and in [33], where nonlinear kinematic hardening with tension-compressoin asymetry has been taken into account for cyclic loading conditions. Further, the Tsai-Hill failure criterion has been used in [184] in an attempt to predict probable locations of failure initiation in wood fibers.

Another important issue is the geometrical description of the fibers including the fiber length, orientation, and thickness distributions. Furthermore, measuring the cross-sections accurately is important for a realistic consideration of single fibers. Nowadays, these geometrical data can be extracted from micro-CT images, see [160, 223] among many others.

2.2 Fiber-Fiber Bonds

In order to properly describe the mechanical behavior of fiber networks, accounting for the fiber-fiber-bonds is crucial [242]. Here, one challenge is determining the actual area of the bonds, which in many cases is much smaller than the analytical contact area [124–126]. Even more, it has been shown in [175] that only 30–40% of the measured overlap area is actually in bonding contact; according to [213], this value varies even in the range from 15 to 88%. However, nowadays, the bonding area is measured through computational image analysis of 3D X-ray microscopy [174, 247] or confocal laser scanning microscopy [150]. In addition, investigations have been made concerning the area in molecular contact in fiber bonds [105] and the corresponding energy contributions of bonding mechanisms [103, 104].

Another even more important aspect is the measurement of force-displacement curves for 2-fiber systems which are usually utilized for investigating the bonding strength. For this, two crossing fibers are considered, one of which is fixed on both ends while the other one is loaded. Different loading cases have been investigated in the literature in order to describe general loading scenarios (see Fig. 1):

1. peeling test (≈ mode I): one fiber is fixed at both ends, the other one is loaded perpendicular to the fiber direction at one end [168, 169, 220];
2. shearing test (≈ mode II): one fiber is fixed at both ends, the other one is loaded in fiber direction at one end [120, 168, 169, 217] (and [121] including the influence of relative humidity);
3. tearing test (≈ mode III): one fiber is fixed at one end, the other one is loaded in fiber direction at one end [81, 169];
4. z-directional test (≈ mode I): one fiber is fixed at both ends, the other one is loaded perpendicular to the fiber direction at both ends [139, 218].

First finite element simulations of the fiber-cross can be found in [241], where both fibers have been modeled orthotropic elastic with simplified cross-sections without lumen. There, comparison between solid and beam elements has shown that the 3D solid elements can provide much more accurate results. Further, first qualitative results for normal traction and shear loadings have been shown in [166]. Based on these investigations, peeling and shearing loadings could be analyzed by using shell elements accounting for the curvature of the fibers [167]. A similar modeling approach has been applied in [71], where resultant forces and bending

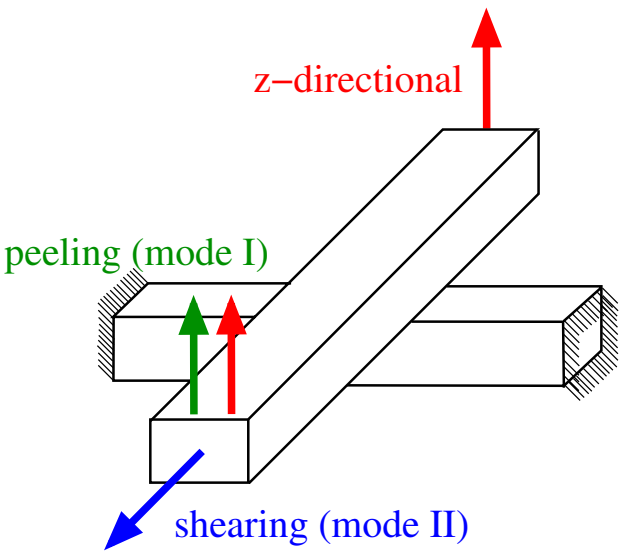

Fig. 1 Different loading cases applied in the fiber-cross experiment

moments have been determined from the peak stresses in all three modes (peeling, shearing, and tearing). Finally, the influence of geometry changes—such as the fiber cross angle and the MFA—on the stiffness of fiber-fiber bonds has been investigated in [39].

In all the works mentioned above, the interface between the fibers has been modeled as perfectly bonded. In contrast, in recent works, the debonding of the fibers is modeled additionally by applying cohesive zone elements [85, 165]. Thereby, the damage progression within the interface can be evaluated until failure of the bond.

2.3 Open Problems on the Fiber Scale

As already mentioned above, the nonlinear single fiber behavior can be taken into account in numerical simulations, as shown e.g. in [33, 203] for elasto-plasticity and in [184] for failure analysis. Nonetheless, precise stress-strain data, that is needed to calibrate such models, is hardly available, yet. This holds even more when the dependence on loading rate, moisture, and temperature is to be considered in addition.

Moreover, obtaining experimental results on the fiber behavior in transverse direction is still an open topic. While the material response in fiber direction can be investigated via uniaxial tension tests, the transversal direction is much harder to test. In principle, the latter can be achieved for example by using AFM nanoindentation for elastic [82] and viscoelastic [62] properties. However, improvements of these methods are still necessary if results shall be used for accurately calibrating the numerical models.

Another critical aspect is the characterization of the cohesive zone models used to describe the debonding of the contact area between fibers. The numerical investigations mentioned above are able to provide an insight into the behavior of the interface and the influence of geometry variations. Nevertheless, the calibration of cohesive zone model parameters—in particular the determination of the critical fracture energies G_{Ic} and G_{IIc}—is still problematic, since the fiber cross experiments are not pure mode tests [3].

3 Modeling Paper on the Fiber Network Scale

As shown in [248], the extensibility of paper relies mostly on three major factors: deformability of the single fibres, the ability of fibres to form strong and flexible bonds, and the three-dimensional structure of fibre network created during the manufacturing process. Hence, models are also needed to characterize the structure of fiber networks.

The first network model for paper has been introduced already in 1952 [60]. Since then, numerous different network models have been developed and applied to paper. These can be classified in several categories: (1) fiber networks that are reconstructed from micro-CT images, (2) structured networks, (3) synthetic networks with random distributions, (4) synthetic networks with statistical distributions.

3.1 Fiber Networks Reconstructed from Micro-CT

One way to generate fiber networks is the reconstruction of real network structures from micro-CT data. In particular, the fiber data as well as the network connectivity data can be analyzed from microtomography images as shown in [35, 251]. Alternatively, in order to avoid the separation of single fibers from the micro-CT images, local and global fiber orientation tensors can be calculated for porous fiber networks given in terms of binarized voxel images. This approach has been employed successfully for thermal conductivity simulations in [221]. Also, a method for determining the number of contacts in a fibrous network based on shortest-path measurements has been developed in [73]. Furthermore, 3D synchrotron X-ray microtomography has been applied to characterize the paper structure of z-structured paper by introducing micro nanofibrillated cellulose in [46]. Finally, the combination of results from synchrotron X-ray 3D microtomography with Mercury intrusion porosimetry (MIP) data has been shown to further improve the information about the considered structures [47].

Clearly, if the network structure is obtained from reconstructing real fiber structures, the results are very close to reality. On the other hand, only very specific structures can be studied without the possibility of varying parameters in a stochastic manner. Thus, it can also be advantageous to generate synthetic network structures for numerical investigations.

3.2 Structured Fiber Networks

One way to generate artificial fiber networks is to use simplified structural designs. For example, a 2D lattice model for simulating the failure of paper has been introduced in [157]. An extension of this lattice model accounting for bond elements and hence three-dimensional effects has been given in [158].

Two-dimensional lattice models based on a periodic (triangular) distribution of spring elements has also been extended already such that interfiber bond failure and subsequent frictional fiber sliding can be evaluated [252]. Such models can also be used as basis of multiscale investigations by simultaneously using the quasicontinuum method, as shown in [23].

Additionally, damage propagation within lattice structures has been investigated based on various criteria of the elimination of overstressed beams. Particularly, a comparison of damage patterns in triangular stretch-dominated and hexagonal bending-dominated lattices can be found in [50], whereas hybrid structures combining both triangular and hexagonal parts are given in [51].

Finally, the elastic-plastic response of 3D fiber networks has been investigated in [164]. While for the analysis of the effect of relative density on the uniaxial yield strength a random fiber network with periodic boundary conditions has been utilized, the dimensional analysis has been performed on idealized transversely isotropic models.

Structured fiber networks are advantageous because they are easy to generate and the computations are relatively cheap. On the other hand, structural and dimensional effects can only be approximated. Therefore, the evaluation of more complex structures can be necessary if structural effects shall be evaluated.

3.3 Random Fiber Networks

In order to allow for statistical evaluations, random fiber networks (RFN) have been generated in multiple ways such that the location of fibers in the network is random. Certain aspects of such random fiber networks can be analyzed by theoretical methods. For example, in [72], a theory has been developed, that describes the statistical properties of rod packings, while taking into account that the deposited rods cannot overlap and thus induce steric hindrances. Further, a new buckling theory including a statistical distribution of free-span lengths has been proposed in [130] and tested against experimental data.

Even so, for most investigations of practical relevance, numerical models need to be established to represent the mechanical behavior of RFN. Since normal paper sheets are mostly formed as highly oriented 2D networks (see e.g. [7]), several attempts have been made to model two-dimensional RFNs. For example, the influence of network deformation and fiber bond fracture on the macroscopic degradation and failure of paper materials has been investigated in [98, 117]. More recently, the mechanical behavior of cross-linked random fiber networks with inter-fiber adhesion have been investigated in tension and compression in [186], where the periodic networks have been created by performing Delaunay and Voronoi tessellations.

However, in order to cover the effects of fiber deformations and fiber bonding, 3D models have proven to be more accurate in many cases. Thus, 3D random fiber networks have been constructed already in [137] to simulate deformation and failure behavior of networks with dynamic bonding/debonding properties using the FEM. Here, the single fibers have been modeled via Tymoshenko beam elements. This approach has been adopted in several recent works. For instance, rotational constraints for 3D beams within random networks have been considered in [179]. Further, accounting for the debonding of fiber-fiber bonds has been performed by use of a cohesive zone model with linear traction-separation law in a penalty-based contact element [34]. The latter formulation has also been applied to examine the effect of changing paramters for the network structure on the short span compression strength [40]. Similarly, the effect of irreversible failure of fibres and of inter-fiber bonds with varying inter-fiber bond density and bond strength has been investigated in [86] for cellulose nanopapers. What is more, in [65], damage accumulation and failure in fiber networks have been examined based on 3D random networks defined on a Voronoi structure, where fibers have been modeled as Timoshenko beams of circular cross-section, while the bonds have been modeled as uncoupled springs with translational and rotational stiffness.

An alternative approach to modeling RFN makes use of the discrete element method (DEM), where each end of fibers as well as each fiber bond are represented by discrete particles, as shown first in [204] for computing the dynamic fracture of thin network materials. Also using the DEM through a series of inter-connected particles in order to generate curly, kinky, and twisted fibers, the creping behavior of soft papers has been explored in [106]. Later, the same approach could be used also to research the uniaxial compression behavior [107]. Lastly, literature results concerning the scaling of elastic modulus as well as strength with increasing density could be reconfirmed in [26] through DEM simulations.

3.4 Statistically Oriented Fiber Networks

If fiber networks are created randomly, the actual distributions of geometrical characteristics are not accounted for. However, these distributions can be incorporated through statistical studies. For example, the fiber lenth distribution has been included in a statistical sense in [140].

Even more important is regarding statistical data on the fiber orientation distribution as shown e.g. in [227] for medium density fiberboards (MDF) made from wood fibers. Extensions of this methodology allowed for the inspection of multilayered structures [226] and of the viscoelastic material behavior of resin-bonded nonwovens [233]. Moreover, the influence of geometrical and spatial effects including the orientation of fibers in the network has been researched in [128], where focus is layed upon the realistic description of crossing fibers. Last but not least, orientation of fibres and positions of bond points in fabrics exposed to stretching in two main orthogonal directions (MD and CD) have been simulated and validated by experiments in [230].

3.5 Open Problems on Fiber Networks

As shown above, random fiber networks for paper have been extensively studied already (see Sect. 3.3). These works are mostly based on DEM or FEM with beam elements, which is computationally very efficient. However, it is not clear how realistic the results can be for out-of-plane loading scenarios. Therefore, comparisons to computations with solid elements as presented in in [140, 149] are advisable.

However, for a more realistic representation of the network behavior, statistical distributions should be considered in addition. Although there are several works dealing with the influence of fiber orientation distributions (see Sect. 3.4) on the overall network response, the majority of these works does not bear on paper but other fibrous networks such as MDF, resin-bonded nonwovens, and nonwovens composed of polypropylene fibers. In consequence, this method needs to be adopted also in the modeling of paper and paperboard with the corresponding statistical distributions and effects. One approach going into this direction has been published recently in [209], where a scheme to identify material parameter distributions using only a limited number of fibres has been developed, which is based on probability density functions (PDF) and Bayesian inference.

Further, it has been shown recently in [136], that local mass density variations play a crucial role, particularly for the fracture behavior of low density papers. Hence, these variations need to be included into the network models additionally.

In addition, the influence of moisture and temperature need to be implemented into the networks models. There exist models for describing the mechano-sorptive creep as result of moisture cycling [237, 238], dimensional instability of networks such as twist due to moisture change [222], as well as for hygro-expansion of the fibers [36–38, 180]. These models are included into random fiber networks. Nevertheless, these are based on idealized structural representations of the bonding between fibers, and thus more sophisticated strategies will be required in the long term.

Another critical issue is the homogenization of the network response to achieve effective properties for the macroscale. The fiber networks considered here cannot be periodized, present an infinite contrast of properties, and include an interconnected porous phase. As shown in [67], that leads to very large ('gigantic') RVE-sizes if only one single RVE is to be investigated. A reduction of the RVE-size is possible if multiple realizations are considered. However, the smallest size of the volume element on the network level that needs to be considered such that the homogenized response is representative in a statistical manner and such that boundary conditions do not affect the result is still not known for paper. While such studies exist for other materials—for instance, for short fiber reinforced elastomers, where at least 4000 fibers should be considered in order achieve a converged RVE-size [48]—they are missing yet for paper and paperboard. First attempts to achieve a converged RVE-size based on numerous computations of multiple realizations have been presented in [8] and [149]. However, no real material parameters for the fibers' nonlinear behavior or the fiber bonds have been included in these works. This is still an open topic for future research.

4 Modeling Paper on the Sheet Scale

On the microscale, paper is a composite that consists of fibers in a network and sourrounding air (see Sect. 3) or can be treated as single pores surrounded by cellulose [214]. In contrast, on the sheet scale, paper can be considered as a homogeneous, anisotropic material that is described in the framework of continuum mechanics. To account for the anisotropic nature, one usually defines three principal directions: machine direction (MD), cross direction (CD), and thickness direction (ZD), see Fig. 2.

Nowadays, such anisotropy is often accounted for by use of the concept of structural tensors [231], which can be applied to problems with large deformations of nonlinear elasticity (see e.g. [210] among many others) and (hyper-) elastic-plasticity [96]. Alternatively, anisotropic 3D material models can be obtained from 1D material models accounting for orientation distribution functions by applying the unit sphere approach suggested in [178], which has already been adapted successfully to model composites with consideration of fiber misalignment [145]. Instead, stochastic continuum models can also be constructed by applying Gaussian fields to the 1D formulation [172]. However, independent of the method utilized, it is crucial to account for the anisotropy of paper on the sheet scale.

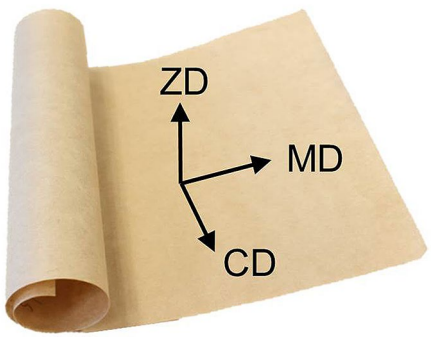

Fig. 2 Definition of principal directions in paper

4.1 Elastic-Plastic Behavior of Paper Sheets

In most models, the assumption is made that the in-plane and out-of-plane behavior can be considered separately; this is justified by the finding that the out-of-plane Poisson's ratio is close to zero, as shown in [234]. Therefore, most elasto-plastic material models for paper are suitable for either the in-plane or the out-of-plane behavior.

An overview of the models described in the following is provided in Table 1.

4.1.1 In-Plane Elasto-Plasticity of Paper Sheets

For the in-plane elastic-plastic behavior of paper sheets, the assumption of small deformations is justified in many technical applications. Then, the basic assumption of an additive split of the total strain into an elastic and a plastic part, $\boldsymbol{\varepsilon} = \boldsymbol{\varepsilon}_e + \boldsymbol{\varepsilon}_p$, can be used. However, if finite deformations (that is finite strains and/or finite rotations) have to be taken into consideration, a multiplicative split of the deformation gradient into an elastic and a plastic part, $\mathbf{F} = \mathbf{F}_e\mathbf{F}_p$.

One way to account for the material anisotropy is applying the concept of an isotropic plasticity equivalent (IPE) material, where the IPE-material is a fictitious isotropic material, subjected to a stress state that equals the corresponding stress state in the actual anisotropic material. This concept, initially introduced in [127] for pressure independent materials, has been applied to paper e.g. in [170]. Recently, this model has been shown to be suitable for predicting results for the box compression test in [163]. In the IPE-model, as in most elasto-plasticity models that have been formulated for pressure independent materials such as metals (see e.g. [42] for an overview), the yield function is given in dependence of the deviatoric stress.

Table 1 Overview of elasto-plasticity models for paper on the sheet scale

Reference	Small/large deformations	Yield function	Hardening	Flow rule	Non-zero parameters
IN-PLANE MODELS					
Xia et al. [253] (XBP02)	Large	Non-quadratic, 6 sub-surfaces	Each direction separately	Associated	23[a]
Mäkelä and Östlund[b] [170]	Small	Non-quadratic	Isotropic	Associated	7
Harrysson and Ristinmaa [97]	Large	Linear + quadratic (Tsai-Wu criterion)	Each direction separately	Non-associated	26
Huang and Nygårds [110]	Small	Quadratic Hill	Linear isotropic	Associated	6
Borgqvist et al. [30]	Large	Based on XBP02	Distortional	Associated	21[a]
Borgqvist et al.[c] [31]	Large	Based on XBP02	Each direction separately	Associated	17[a]
Tjahjanto et al.[c] [240]	Small	Based on XBP02	Each direction separately + kinematic	Associated	28[d]
Wallmeier et al. [250]	Small	Four separate functions	Linear, each direction separately	Associated	9[e]
Li et al. [146]	Small	Based on XBP02	Isotropic + kinematic	Associated	10[a]
Bedzra et al. [20]	Small	Three separate functions	Each direction separately	Associated	12[a]
Pfeiffer and Kolling [205]	Small	Quadratic	Each direction separately	Non-associated	24[a]
OUT-OF-PLANE MODELS					
Stenberg [236]	Small	Bounding surface	Separately for compression/shear	Non-associated	9[f]
Nygårds [188]	Small	Two separate functions	Separately for compression/shear	Associated	5[g]
Borgqvist et al. [31]	Large	Based on XBP02	Only in ZD compression	Associated	8[f,h]
Tjahjanto et al. [240]	Small	Based on XBP02	Densification	Associated	15[f,h,i]
Li et al. [147]	Large	Based on XBP02	Only in ZD compression	Associated	8[f,i]

[a]Including plastic strain ratios in CD and MD

[b]For the plane stress constitutive relation that is derived from the more general case

[c]For the in-plane part of the presented model

[d]Including plastic strain ratios in CD, MD, 45°; without counting the viscoelastic parameters

[e]Without counting the thermal parameters

[f]Including the internal friction coefficient

[g]Without counting the parameters of the interface model

[h]In addition to the parameters of the in-plane model

[i]Including the plastic parameters for densification in compression

Since this might no be realistic for paper, numerous alternative models have been invented specifically for paper.

Another way to include anisotropy into the elastic-plastic model is the use of an orthotropic yield function that accounts for different yield stress values in different preferential directions. The most common one is the formulation of Hill [102], that includes six yield stress values. In particular in forming processes such as creasing and folding, this model has been applied successfully e.g. in [90, 109, 110] amongst others (see also Sect. 7). Additionally, Hill's yield function has been utilized for the simulation of the box compression test [254] and of lateral compression tests of layered paperboard tubes [61].

Further, a well-known model for the in-plane elastic-plastic material behavior of paper is the one presented by Xia et al. in [253]. Here, the assumption is made that the out-of-plane material response is purely elatic, such that the plasticity model is not affected by any stress component that refers to ZD. Then, the yield surface can be defined as the sum of six sub-surfaces, four of which describe the tension and compression in MD and CD, respectively, whereas the remaining two surfaces correspond to positive and negative shear, respectively. As shown in [192, 193], this model captures the in-plane response of paper in creasing and folding very well, while the out-of-plane behavior should be modified to also account for delamination in thickness direction. Noteworthy, the formulation of [253] and [193] has already been implemented into LS-DYNA as `*MAT_PAPER` as material type 274 [219].

A modification of the model of Xia et al. [253] has been presented in [30]. There, the yield function has been taken over from the original model but the harding part has been modified such that a coupling between the hardening of the six different sub-yield surfaces is introduced, allowing for non-isotropic hardening. Based on this work, in [31], a similar formulation has been developed that included hardening in tension and shear, while ideal plasticity was assumed in compression. Furthermore, in order to consider also viscous effects in model, the formulation of Xia et al. has been extended in [240] accounting for strain-rate dependent material behavior. Even more, also the densification in thickness direction has been incorporated (see Sect. 4.1.2) and the hardening model has been extended to be anisotropic-kinematic without introducing additional parameters. Another variant of the Xia et al. model has been provided in [146], where—as in the latter one—a small strain formulation has been derived including both isotropic and kinematic hardening in order to account for the anisotropic nature of hardening behavior. In addition, an alternative small-strain version of the Xia et al. model has been suggested recently in [205], where focus is laid on introducing a non-associated flow rule.

Moreover, the yield criterion can be formulated based on the Tsai-Wu criterion, which consists of a linear combination of quadratic and linear function in stress. This criterion has been applied in [97] for modeling the in-plane behavior of paper successfully. Moreover, based on a previous investigation [96], the flow rule has been formulated in a non-associated manner.

Finally, it is also possible to account for the material's anisotropy by defining several different yield functions in the framework of multi-surface plasticity. For example, in [250], four different yield functions have been defined depending on whether MD or CD loading is dominant and discriminating between tension and compression. The formulation is simple, only requires a relatively low number of parameters, and includes even thermal dependence of the mechanical parameters. Another model based on multi-surface plasticity has been recently derived in [20], where three distinct yield functions are applied to distinguish between normal loading cases in MD and CD, respectively, as well as shear loading. It has been pointed out that the results are similar to the ones obtain from a model with one single non-quadratic yield function.

4.1.2 Out-of-Plane Elasto-Plasticity of Paper Sheets

In many technical applications, the out-of-plane response of paper is relevant, too. Consequently, several models have been invented also for elasto-plasticity in thickness direction.

For instance, based on experimental findings [235], a small-strain model has been suggested in [236], in which the nonlinear elastic behavior has been treated by accounting for the porous nature of the material as well as the plastic response under high compressive loads in ZD direction through defining a bounding surface.

The different material behavior in compression and shear can also be tackled by the concept of multi-surface plasticity. In particular, two separate yield functions with corresponding separate hardening laws have been introduced in [188]. One of the two functions represents compressive stresses in ZD while the other refers to shear.

To this author's best knowledge, there are only two publications available in literature, in which in-plane elasto-plasticity models have been extended such that also the out-of-plane direction is treated. The first one is [31], in which the yield function of Xia et al. is augmented by six additional sub-surfaces to include all ZD-loading components. The model is based on the assumption that the fiber-layer normal direction remains unchanged during out-of-plane shear deformations. Hardening is only active for ZD compression, whereas all other out-of-plane plastic deformations are modeled as ideal plastic. Similarly, also in the second work [240], the yield function of Xia et al. is expanded such that in total 14 sub-surfaces are considered. An important

aspect in this model is accounting for the material through-thickness densification in both the elastic and the plastic parts of the model.

Finally, the densification effect has also been addressed in [147]. This formulation is thermodynamically consistent and valid for finite deformations. It includes three sub-surfaces in the yield function. As in the model of [31], hardening only occurs for ZD compression. Also, the internal friction effect is taken into consideration such that the plastic response in compression and shear is coupled.

4.2 Modeling Viscous Effects in Paper Sheets

It is a well-known fact that paper shows rate-dependent material behavior and viscous effects [95] because of the hygroscopic nature of the fibers (not the bonds [64]). Particularly the creep and relaxation behavior are of high significance and have thus been subject to extensive studies—see e.g. the overview provided in [55].

In the last years, experimental studies on the creep behavior of paper have mostly focused on its influence on the compressive strength of corrugated paperboard packages. For example, in [78], box compression tests as well as creep compression tests have been performed. Amongst others, it has been found that refrigerated conditions increased the creep rate of the packages in comparison with the standard conditions. In addition, the mechanosorptive effect, which describes the combined action of mechanical creep loading and changing moisture content, has been included into testing procedures in [114] and [134, 135]. In these works, testing has been executed in climate chambers that allowed for controlled cyclic changes of relative humidity leading to accelerated creep. Concerning relaxation, the effects of strain rate on the tension-strain curve and relaxation of wet paper have been researched in [133]. Further, both the creep [183] and relaxation [182] behavior have been studied recently with the help of a folding experiment that has been performed on creased paperboards.

One way to model the mechanosorptive effect is to consider the stresses that are produced by moisture content changes in the constraint fibers of the underlying network [6, 237, 238]. For instance, in [6], from the relations derived on the network level, a rheological model with springs and dampers has been developed that allows the description of creep via a continuum model. However, no structural problem has been considered.

There are only few works in which the viscous effects have been tackled also on the structural level by means of finite element simulations. In [207], this is performed for corrugated paperboard in two steps: The transient analysis has been conducted first in order to calculate the relative humidity values as a function of time, and the second stage of the analysis has been calculating the fiberboard deformation response (hygroexpansion) due to the change in relative humidity values. Creep is incorporated through a simple creep equation that relates the strain to stress and time.

Besides, the effect of the through-thickness moisture content gradient on the moisture accelerated creep has been simulated by using an isotropic hygro-viscoelastic model in [229]. It has been shown that the rate of the moisture content change and the steepness of the gradient affect the creep rate greatly. In addition, based on these results it has been suggested that the internal stresses generated by hygroexpansion may increase the creep rate when material layers with different moisture content exist.

Alternatively, the relaxation behavior can also be included to the model by directly affecting the internal stress decrease. This has been done in [75, 142] in combination with a simple plasticity model with von Mises yield criterion for plane stress states to capture cyclic and irreversible straining phenomena.

Furthermore, the multi-surface plasticity of Xia et al. (2002) [253] (see Sect. 4.1) has been extended to viscoelastic and viscoplastic behavior in [240]. For the viscoelastic model, the generalized Maxwell model has been adopted, such that the stress is split additively into the steady-state and the transient parts, where the transient stresses are computed from simplified integral expression accounting for the elastic strain rate. For the viscoplastic model, in order to account for time- or rate-dependent plastic deformation, a Perzyna-type power-law kinetic relation is introduced for the viscoplastic strain evolution. Applications of this viscoelastic viscoplastic model to compressive creep and compressive relaxation in thickness direction can be found in [84].

4.3 Modeling Effects of Temperature and Moisture in Paper Sheets

In the previous section, the influence of moisture on the material behavior of paper has partly been described already, because it has a significant effect on the creep behavior. However, the dependence on moisture and moisture change has been studied as a separate topic in several works. An overview about the factors affecting the hygroexpansion of paper is provided in [151], where mostly the fiber and the network level are addressed. However, numerical models are not discussed in detail at all.

The moisture transport in cellulose-based materials can be modeled using the framework of porous materials. For instance, a theoretical water vapor transport model has been developed for cellulose-based materials in [19] based on the assumption of isotropic material properties. Further, a steady-state finite element model of moisture transport in corrugated fibreboard has been presented in [41], where

values of moisture permeability have been determined experimentally. Finally, also on the sheet level the moisture adsorption can be described, as has been conducted in [27] using a computational fluid dynamics (CFD) model. However, in the latter models, no coupling to the mechanical behavior has been conducted.

One way to do account for the moisture dependence of the mechanical material response on the sheet level is through homogenization of network simulations [37, 38, 246]. The corresponding fiber networks have been generated randomly (see Sect. 3.3), whereas idealized geometries have been studied for the hygroexpansion. Another strategy to investigate the effect of moisture diffusion on the microstructure has been presented recently in [123]. The model established therein is based on 2D scanning electron microscope images of real microstructures for describing moisture transport in paper sheets in order to explain the time-dependent natural aging process of a paper sheet and book stacks.

As an alternative, the moisture-dependence can be implemented directly into the continuum model approach on the sheet scale in a phenomenological sense. For example, the moisture induced out-of-plane deformation of a paper sheet has been investigated in [143], where elastic behavior assumed and anisotropy is taken into account. Moreover, in a similar approach to the already mentioned works [75, 142] (see Sect. 4.2), an elastio-plasticity model has been adopted in [156] for the plane stress case, where the yield point as well as the hardening have been formulated as functions of both the anisotropy and the dry solids content.

The other very important factor influencing the mechanical behavior of paper is temperature. One thermo-mechanical simulation has been undertaken in [250] for the deep-drawing process of paperboard. In particular, one of the relevant process parameters to be varied has been the die temperature. To include the temperature dependence into the deep drawing simulation, the mechanical parameters have been treated as functions of temperature.

However, in many applications with high temperature variations, also the moisture change is not negligible. Then, the combined effects of moisture and temperature on the mechanical response of paper have to be captured [152]. This is true e.g. for printing processes of paper, which are therefore subject to several examinations. For example, the coupled heat and moisture transport problem has been tackled in [256], where the considered paper sheet has been moving over a warm print surface. Likewise, in [141], a mathematical model of moisture and heat transport has been derived and applied to a paper sheet that moves through a fusing nip in a printer.

Another process, in which both moisture and temperature play crucial roles, is hydroforming of paper. That process has been modeled in [154] using the simple elasto-plasticity model derived in [250] mentioned above. In this work, the material parameters are defined as functions of moisture as well as temperature. However, the problem has not been solved in a completely coupled manner, but instead some key assumptions have been made, which allow the drying effect to be captured within the framework of the material model without the need of an external solver for the moisture gradient.

Additionally, the heat and moisture transport can be relevant during storage of paper rolls, which has been treated in [5]. In this work, a macroscopic three-phase model—consisting of solid fiber, bound water, and pore gas—has been derived to describe transport and mass exchange processes in paperboard. Governing equations have been obtained through simplification of the general field equations: mass conservation, linear momentum, and energy conservation, established in the hybrid mixture theory framework. Similarly, a three-phase model has also been introduced in [10], where a two-scale framework has been employed. The resulting model has been applied [12] to failure analysis of moist packaging material exposed to excessive heating and in [11]—in combination with an anisotropic elasto-plasticity model taken from [31]—to investigate the response of paperboard in conditions similar to those present during a local sealing of two sheets of paperboard.

Concluding, an overview of the models that have been implemented into mechanical structural analyses (FEA) is provided in Table 2.

4.4 Damage Progression in Paper Sheets

Predicting the failure of paper and paperboard is relevant for improving the material performance. Here, the effect of different loading scenarios is of particular interest. These can be examined experimentally for example by using inflation tests [29] or biaxial in-plane tensile testing [153]. In both of these works, the experimental results on the failure of paper have been transfered into mathematical models by defining failure surfaces, where in [153] both stress-based and strain-based surfaces have been analyzed. However, even before the final failure state is reached, significant damage progression can be observed in paper and paperboard. This evolving damage leads to reduction of the stiffness, as shown experimentally e.g. in [99].

Recent experimental investigations focus on local effects on the damage behavior. For example, in [138], local structural properties have been measured and put in relation to local tensile deformations, which due to accumulation may yield to initializing the failure of paper. Further, the effect of small-scale deformations caused by mechanical treatment (refining) of pulps on the tensile behavior of fibers and papers has been studied in [132].

From modeling point of view, it is also possible to describe the damage progression on the fiber or network

Table 2 Overview of time-/rate-, moisture-, and temperature-dependent models for paper on the sheet implemented into mechanical structural analyses (FEA)

References	Plasticity	Time-/rate-dependent	Moisture-dependent	Temperature-dependent
Leppänen et al. [142]		Relaxation	Anisotropic	
Rahman et al. [207]		Creep	Isotropic	
Lipponen et al. [156]	Based on Hill (2D)		Anisotropic	
Erkkilä et al. [142]	Based on [156] (2D)	Relaxation	Anisotropic	
Tjahjanto et al. [240]	Based on XBP02	Viscoelastic−viscoplastic		
Wallmeier et al. [250]	Four separate functions			Dependent parameters
Girlanda et al. [84]	Based on [240]	Compressive creep and relaxation		
Linvill & Östlund [154]	Based on [250]		Dependent parameters	Dependent parameters
Askfelt and Ristinmaa [12]	Based on [31]		Coupled, anisotropic	Coupled, isotropic
Leppänen et al. [142]	von Mises (2D)	Relaxation	Isotropic	

level in order to account for localized effects. One way to do that is establishing a relation between the fraction of broken bonds on the network scale—which represents the degree of material degradation—and the reduction of the network's macroscopic stiffness [98, 116]. More recently, computations of deformation and damage in random fiber networks (see also Sect. 3.3) can be found, for instance, in [230].

Nevertheless, it is more convenient to model damage evolution in a continuum sense on the sheet scale. For this, the classical approach consists of introducing a damage variable D, which controls the material degradation in a continuous fashion. Since this damage variable is treated as an internal variable, an evolution equation needs to be defined in order to describe how the damage evolves under the current loading path. Such evolution equations can be defined either phenomenologically—as done in [115], where the damage evolution law is defined in dependence of the damage energy release rate—or based on microstructural observations on the network level [99].

One important issue is the modeling of continuum damage in an anisotropic manner, since the material response of paper is strongly anisotropic. One way to achieve an anisotropic formulation is the introduction of more than one scalar-valued damage variables (see e.g. [225] for details concerning composites in general). Particularly for paper, three different damage variables can be introduced in order to discriminate the behavior in MD, CD, and ZD [118]. Further, in [49], several differents fiber sets have been considered on the network level, where for each fiber set a scalar damage variable has been defined. As an alternative, a second order damage tensor can be introduced such that a tensor-valued evoltion law needs to be defined [206].

Finally, it should be mentioned that continuum damage models generally suffer from pathelogical mesh dependence. In order to obtain mesh-independent results, viscous regularization of Perzyna-type can be applied, as shown in [206]. Alternatively, non-local models, in which non-local quantities are incorporated into constitutive equations can preserve mesh-independence [49, 99, 118].

4.5 Open Problems on Sheet Level

Concerning the elasto-plasticity models, one major challenge is the combination of in-plane and out-of-plane material behavior. Even though there are models that take both into account [2, 31, 240], not all physical effects are captured by these models, yet. Moreover, one particular challenge is the determination of material parameters. As can be seen from Table 1, the more effects the models can cover, the more parameters are usually involved that need to be calibrated. Even though several strategies for parameter identification exist, see e.g. [187], there is still a need for more sophisticated experimental methods. In particular, the transverse shear properties are still difficult to get by direct measurement [101, 190].

One additional aspect, that has not been accounted for in elasto-plasticity models for papers is the plastic volume change that accompanies the densification effect. As shown in [239], this plastic volume change should be incorporated into the definition of the energies through J_p and hence considered in the Clausius-Duhem inequality. While this issue has been accounted for in models for other elastic-plastic materials—such as geomaterials [24, 25]—it has not been considered for paper, yet.

What is more, the combination of viscoelastic-viscoplastic models with mechanosorptive creep—as developed already for other materials such as wood [211, 212]—still needs to be applied to paper and paperboard. Even more, the fully coupled solution of the time-, rate-, moisture-, and temperature-dependence has not been achieved, yet. This is already challenging and computationally expensive in the isotropic case. However, the moisture and temperature

transport might even be necessary to be described in an anisotropic fashion.

Furthermore, the coupling of the aforementioned effects with the continuum damage modeling of paper has not yet been tackled. Besides, the existing damage models for paper are limited to small deformations. Hence, there is a strong need to fill this gap by extending existing modeling strategies for the finite deformation regime.

5 Modeling of Paperboard Laminates

Paperboard is often used in packages. Then, usually laminates of several layers with different properties are applied. In principle, either the whole laminate can be modeled in a smeared manner with just one effective material model—see e.g. [195] for a recent application to modeling the drop test and compression test of a gable top package—or each of these layers can be described by the models presented in the previous section. In addition, several different materials are often applied that influence the overall performance of the laminate. For example, the softening of the aluminum foil which prevents light and oxygen penetration in beverage packaging can be considered [28, 29, 255].

Anyways, one additional aspect that should be given consideration is the interface behavior between the layers. This can be done by introducing cohesive zone models (CZM), that describe the softening behavior during delamination via the definition of a traction-separation law, in each interface between layers. In the simplest case, the layers can be modeled with a linear elastic continuum mechanical model, while the bonding between the layers is considered via a CZM [93]. There, an orthotropic elastic-plastic cohesive law has been incorporated through an additive split of the separation into an elastic and a plastic portion. A similar interface model has also been used in [188] in combination with an elastio-plasticity continuum model for the layers. Likewise, such a model has been implemented already into LS-DYNA as `*MAT_COHESIVE_PAPER` as material type 279 [129].

Classical cohesive zone relations for composites use bilinear traction-separation laws, see [43, 224, 245] to name only a few, but also more complex laws exist—such as trilinear [1, 89], quadratic [74], square root [228], exponential [161, 185], and general power laws [108, 202]—for special applications, e.g. when fiber bridging occurs. In contrast, in paperboard applications, the majority of traction-separation relations are exponential [21, 94, 144, 171, 188, 244], and less works use bilinear ones [58, 59]. Alternatively, the tranction-separation relations can also be defined directly from experimental results from fracture mechanics tests by evaluating the critical J-integral [257, 258].

In most technical applications, the loading of the interface is not only pure peeling (mode I), pure shearing (mode II), or pure tearing (mode III). Instead, combinations of these loadings occur in the interface that delaminates. Consequently, one relevant aspect for cohesive zone modeling is taking such mixed-mode loading cases into account. This can be achieved by defining traction-separation laws based on effective quantities [21, 94, 188]. However, when mixed-mode scenarios are considered, it is essential to prove consistency of the chosen traction-separation laws for any possible loading path, because otherwise non-physical results can be obtained as shown in [66, 200]. To overcome these issues and to guarantee thermodynamic consistent results, cohesive model formulations should be based on potentials that couple the behaviors in different modes in a consistent manner. For example, the potential developed in the PPR-model [45, 201, 232] can be adapted to paperboard applications, as shown in [144]. Similarly, a new mixed-mode framework has been proposed in [58, 59] in which the unilateral effect is accounted for and interpenetration upon interface closure is prevented.

An additional challenge is the calibration of these models. The classical experimental tests that can be conducted to measure the delamination resistance of paper and board include the Scott bond test [80, 119], the z-directional testing based on lamination techniques [9, 79], the Y-peel test [94], and the short-span uniaxial tension tests [243]. The aforementioned procedures are useful for the out-of-plane tensile response. The corresponding shear response is even harder to investigate. For this, the notched shear test (NST) has been invented [191, 194]. In addition, the short-span compression test can be interpreted such that conclusions on the shear properties can be drawn [91, 101].

An alternative approach is adapting test setups, that have been initially developed for fiber-reinforced composites, to paper and paperboard. For example, the mode I behavior has been investigated based on the double cantilever beam (DCB) test in [59, 144, 148], while the mode II response has been analyzed based on the three-point (3ENF) [144, 148] and four-point (4ENF) [59] end-notched flexure tests. For mixed-mode loadings, the use of mixed-mode bending (MMB) tests has been suggested in [58], but actual tests have not been conducted. Alternatively, a non-proportional separation test has been performed in [144]. Even so, accurate and reliable measurements for the mixed-mode behavior of paperboard are still an unsolved problem.

6 Modeling of Corrugated Paperboard

Packaging boxes are often formed from corrugated paperboard, i.e. by gluing fluted sheets of paperboard as core material to flat face sheets of linerboard. When these

materials are modeled, this specific structure needs to be addressed.

One important issue is the influence of creasing on the overall behavior of the corrugated paperboard. For example, in [97], it has been shown that the creases result in local reduction of the bending stiffness, which is desirable because it simmplifies the folding operation. Therein, creasing of a corrugated board panel has been modeled by letting a punch deform the liner and fluting elasto-plastically.

A most relevant property of boxes made from corrugated paperboard is their compression strength. One way to quantify the box compression strength is by performing box compression tests (BCT). Already in the 1960's, such tests have already been performed and evaluated by analytical methods, such as the McKee equation proposed in [176]. Some more recent observations on this model, its implications, and possible improvements can be found in [56].

Nowadays, however, most predictive models for simulating the BCT are based on the finite element method. For instance, the critical buckling loads have been distinguished using an orthotropic elasto-plasticity model in [254], where different geometries and the influence of creases have been considered. In addition, the influence of material orientation has been analyzed in [163] by comparing boxes that were cut to have compression axes along MD and CD, respectively. What is more, the BCT has also been described numerically in [78]. There, also the compressive creep behavior of ventilated corrugated paperboard packages has been accounted for by changing loads as well as environmental conditions.

Another test to determine the compression strength is the edge crush test (ECT). This test has been investigated by FEA e.g. in [100], where plasticity was defined by Hill's model and failure by the Tsai-Wu criterion. Also, corrugated paperboard samples have been researched in the ECT and boxes from the same material in the BCT in [76], where only linear elastic material behavior has been assumed. Finally, the ECT has also been examined in [134, 135] using a new test rig and comparing to simulations. The setup allowed to subject the specimen to cyclic climate change in a climate chamber, thereby triggering creep behavior.

Further, the influence of humidity and moisture on the material response of corrugated paperboard has been in focus of research. For example, the humidity effect on compressive deformation and failure of recycled and virgin layered corrugated paperboard structures has been investigated in [181]. Also, the steady-state moisture transport through corrugated fiberboard packaging has already been explored in [41]. Aside from that, the influence of moisture loading cycles in terms of accelerated creep has been surveyed in [114].

Until now, the question of sustainability of corrugated paperboard and the corresponding manufacturing processes has not catched a lot of attention, yet. This is suprising, since corrugated paperboard is an energy-efficient material which is reusable, fully recyclable, and simple to produce. In consequence, the carbon and water footprints of corrugated board are less than of any other packaging material [44]. Nonetheless, the supply chain and its environmental impact is not well investigated, yet. In fact, to the knowledge of this author, the only work in this field is [69]. In consequence, much more effort needs to be invested in this topic as is done for other packaging processes, see e.g. the review [177] and the references therein.

Lastly, also alternative paperboard sandwich structures could be evaluated. For example, crumpled papers have been investigated in [173], and it has been shown that these exhibit mechanical properties that are comparable to flexible and rigid commercially-available polymer or aluminum foams of similar densities. Thus, this could be an interesting material for substituting core materials of paperboard sandwich structures.

7 Modeling of Forming Processes with Paperboard

Several forming processes of paper and paperboard have been explored by numerical models. From these, a brief selection is described in the following. A more complementary review on these forming processes is provided in [198], while an overview with special focus on creasing and folding is given in [57].

7.1 Creasing and Folding

Two important converting processes in the forming of laminated paperboard to packages for products are creasing and folding. Creasing is the manufacture of fold lines such that the bending stiffness of the board is reduced preventing it from breaking during the following folding step. For this, delamination is introduced between the layers.

There exist numerous works in the literature on creasing and folding, in which the layers are modeled with relatively simple elastic-plastic material models. For example, Hill's yield function has been applied for the paperboard layers of coated paperboard in [16, 17], whereas the coating layers have been modeled using the von Mises yield criterion for ideal plasticity.

As already mentioned above, delamination plays a crucial role in the creasing and folding processes and thus should be considered also in the numerical models. This can be achieved conveniently by cohesive zone formulations as shown e.g. in [21], where the orthotropic Hill model with isotropic strain hardening has been applied for the layers, while a cohesive zone model with normal and shear

components has been introduced for the interfaces. The latter modeling approach has also allowed investigating the influence of the delamination description and different numbers of delamination surfaces [22].

In addition, the cohesive behavior can also account for differences in MD- and CD-direction by introducing two different shear components as shown in [110, 111]. With the help of this modeling strategy, numerical simulations could be performed with different shear strength profiles of the considered laminates by altering the ply and interface properties. Thereby, different production strategies could be mimiced. It was shown that the interface strengths mainly influenced the folding behavior, whereas the ply properties mainly affected the creasing force [109]. Further, the delamination during the folding of creased paperboard has been modeled in [83] through a special interface element with both, elasto-plastic as well as damage behavior.

In other works on creasing and folding of paperboard, more complex material models have been used. For instance, the anisotropic elasto-plasticity model of Xia et al. [253] has been adopted for the in-plane behavior of the paperboard layers in [192, 193], while the out-of-plane behavior has been treated through a cohesive interface model. Alternatively, the elastic-plastic model of [31] has been inserted in the simulation of the line folding process in [32]. Moreover, in [54] the orthotropic elastic-plastic material response has been described on the basis of the Ramberg-Osgood plasticity model [208], where the strain in MD oder CD, respectively, is defined as function of stress via a power law. Moreover, in order to account for the tension-compression asymetry, the isotropic plastically unsymmetric Drucker-Prager model [70] with extensions proposed in [199] has been adopted in [68] for creasing and folding simulations. Finally, a finite element analysis of the folding process of creased white-coated paperboard has been performed in [122] using a combined fluffing resistance and shear yield glue model.

Although a lot of work has been done concerning the modeling of creasing and folding of paperboard, there are still several open issues. In general, the material models used are relatively simple in most cases. Thus, more complex phenomena such as creep and relaxation have not been included yet into the simulations, although the effects have been shown experimentally to be influential [182, 183]. Further, deeper investigations concerning the optimization of the shear strength profile should be undertaken [189] and potential improvements to increase the peak bending angle in folding should be developed, e.g. by using a needled middle layer [131]. Last but not least, more sophisticated comparisons with results of alternative testing setups such as the Scott Bond Test could yield deeper insigth into the processes [63].

7.2 Forming and Deep-Drawing

The forming and deep-drawing of paperboard is a relevant field of research, because these processes differ significantly from applications in sheet metal forming [87]. Nevertheless, only few works are available in the literature, yet.

There are three main methods for producing advanced shapes of dry paper and paperboard [92]. While in press-forming a solid male and female die are used to convert the paper, in hydro-forming the male die is substituted by a pressurized membrane. In contrast, a male punch is pushed through a whole during deep-drawing.

One important converting process is press-forming, which is particularly suitable to produce deep trays. In order to evaluate the resulting creasing patterns that are produced during the converting, an orthotropic elastic-plastic model based on Hill's yield criterion has been applied in [14]. An extension of the latter model to predict failure has been given in [15]. In addition, the delamination behavior has an important effect on the modeling of the forming process, as shown in [112].

The hydro-forming process has also been investigated via finite element analysis. For example, in [88] the isotropic elastic-plastic von Mises criterion has been applied. More complex material behavior has been implemented for instance in [154], where both the moisture- and the temperature-dependence have been accounted for. The comparison between press-forming and hydro-forming can be found in [92].

What is more, the deep-drawing process has been modeled with an explicite FEA in [250]. A statistical approach has been applied additionally in [249] in order to include the occurrence of rupture. Furthermore, wrinkle prediction as well as the post-wrinkle behavior have been included into the model in [155].

Lastly, the simulation of the packaging forming process is provided in [215]. There, anisotropic elastic-plastic model presented in [31, 32] has been applied successfully to the large-scale formin of a packaging product. The material model has been implemented into a solid-shell finite element formulation such that the thin, shell-like structure could be considered using the fully three-dimensional material model.

8 Conclusions

Paper and paperboard are characterized by their multi-scale and multi-physics nature, since several different physical effects can be observed on different scales. Further, the material behavior is nonlinear and anisotropic as well as dependent on time, loading history, strain rate, temperature, and moisture. Additionally, in most cases, large rotations and strains have to be considered. In consequence, all

these aspects have been included into models for paper and paperboard. Nonetheless, it can be concluded that no model exists yet, that is capable of accounting for all these effects simultaneously.

Moreover, the forming processes that are applied to paperboard products include very complex structural steps with complicated loading states. Therefore, simplified models have been used frequently in order to minimize the computational effort. Although these simplified approaches are necessary for simulations of structures with practical relevance, the more complex multi-scale and multi-physics models have to be further developed to enable engineers to further optimize the material properties and the forming processes. Only then, the field of applications of paperboard can be extended to other branches such as building construction [13, 162] or electrical engineering [197].

Acknowledgements Open Access funding provided by Projekt DEAL. Parts of this paper have been written during a research stay at Columbia University. Thus, the hospitality of Prof. Jacob Fish is kindly acknowledged as well as the funding provided by the German Research Foundation for this cooperation (Deutsche Forschungsgemeinschaft DFG, Project Numbers SI 1959/5-1 and SI 1959/7-1).

Compliance with Ethical Standards

Conflict of interest There is no conflict of interest.

References

1. Airoldi A, Dávila CG (2012) Identification of material parameters for modelling delamination in the presence of fibre bridging. Compos Struct 94:3240–3249
2. Alajami A, Li Y, Simon JW (2018) Modelling the anisotropic in-plane and out-of-plane elastic-plastic response of paper. Proc Appl Math Mech 18:e201800322
3. Alajami A, Li Y, Kloppenburg G, Simon JW (2019) Evaluating the mechanical response of fiber networks with RVEs. In: Proceedings of the international paper physics conference, pp 51–56
4. Alava M, Niskanen K (2006) The physics of paper. Rep Prog Phys 69:669–723
5. Alexandersson M, Askfelt H, Ristinmaa M (2016) Triphasic model of heat and moisture transport with internal mass exchange in paperboard. Transp Porous Med 112:381–408
6. Alfthan J, Gudmundson P (2005) Linear constitutive model for mechano-sorptive creep in paper. Int J Solids Struct 42:6261–6276
7. Alimadadi M, Uesaka T (2016) 3D-oriented fiber networks made by foam forming. Cellulose 23:661–671
8. Andrä H, Edelvik F, Fredlund M, Glatt E, Kabel M, Lai R, Mark A, Martinsson L, Nyman U, Rief S (2011) Micromechanical network model for the evaluation of quality controls of paper. Progr Pap Phys Semin 8:49–55
9. Andersson C, Fellers C (2012) Evaluation of the stress–strain properties in the thickness direction—particularly for thin and strong papers. Nordic Pulp Pap Res J 27:287–294
10. Askfelt H, Alexandersson M, Ristinmaa M (2016) Transient transport of heat, mass, and momentum in paperboard including dynamic phase change of water. Int J Eng Sci 109:54–72
11. Askfelt H, Ristinmaa M (2017) Response of moist paperboard during rapid compression and heating. Appl Math Model 42:114–132
12. Askfelt H, Ristinmaa M (2017) Experimental and numerical analysis of adhesion failure in moist packaging material during excessive heating. Int J Heat Mass Transf 108:2566–2580
13. Auslender A, Biesalski M, Groche P, Knaack U, Schneider J, Schabel S (2017) Building with paper: new applications for a diverse material. Wochenblatt für Papierfabrikation 145:822–824
14. Awais M, Sorvari J, Tanninen P, Leppänen T (2017) Finite element analysis of the press forming process. Int J Mech Sci 131—-132:767–775
15. Awais M, Tanninen P, Leppänen T, Matthews S, Sorvari J, Varis J, Backfolk K (2018) A computational and experimental analysis of crease behavior in press forming process. Proc Manuf 17:835–842
16. Barbier C, Larsson PL, Östlund S (2005) Numerical investigation of folding of coated papers. Compos Struct 67:383–394
17. Barbier C, Larsson PL, Östlund S (2006) On the effect of high anisotropy at folding of coated papers. Compos Struct 72:330–338
18. Batchelor W, He J (2005) A new method for determining the relative bonded area. Tappi J 6:23–28
19. Bedane AH, Eić M, Farmahini-Farahani M, Xiao H (2016) Theoretical modeling of water vapor transport in cellulose-based materials. Cellulose 23:1537–1552
20. Bedzra R, Li Y, Reese S, Simon JW (2019) A comparative study of a multi-surface and a non-quadratic plasticity model with application to the in-plane anisotropic elastoplastic modelling of paper and paperboard. J Compos Mater 53:753–767
21. Beex LAA, Peerlings RHJ (2009) An experimental and computational study of laminated paperboard creasing and folding. Int J Solids Struct 46:4192–4207
22. Beex LAA, Peerlings RHJ (2012) On the influence of delamination on laminated paperboard creasing and folding. Philos Trans R Soc A 370:1912–1924
23. Beex LAA, Peerlings RHJ, Geers MGD (2014) A multiscale quasicontinuum method for dissipative lattice models and discrete networks. J Mech Phys Solids 64:154–169
24. Bennett KC, Regueiro RA, Borja RI (2016) Finite strain elastoplasticity considering the Eshelby stress for materials undergoing plastic volume change. Int J Plast 77:214–245
25. Bennett KC, Regueiro RA, Luscher DJ (2019) Anisotropic finite hyper-elastoplasticity of geomaterials with Drucker-Prager/Cap type constitutive model formulation. Int J Plast 123:224–250
26. Bergström P, Hossain S, Uesaka T (2019) Scaling behaviour of strength of 3D-, semi-flexible-, cross-linked fibre network. Int J Solids Struct 166:68–74
27. Berry TM, Ambaw A, Defraeye T, Coetzee C, Opara UL (2019) Moisture adsorption in palletised corrugated fibreboard cartons

under shipping conditions: a CFD modelling approach. Food Bioprod Process 114:43–59
28. Bolzon G, Cornaggia G, Shahmardani M, Giampieri A, Mameli A (2015) Aluminum laminates in beverage packaging: models and experiences. Beverages 1:183–193
29. Bolzon G, Talassi M (2014) Aluminum laminates in beverage packaging: models and experiences. Compos B Eng 66:358–367
30. Borgqvist E, Lindström T, Tryding J, Wallin M, Ristinmaa M (2014) Distortional hardening plasticity model for paperboard. Int J Solids Struct 51:2411–2423
31. Borgqvist E, Wallin M, Ristinmaa M, Tryding J (2015) An anisotropic in-plane and out-of-plane elasto-plastic continuum model for paperboard. Compos Struct 126:184–195
32. Borgqvist E, Wallin M, Tryding J, Ristinmaa M, Tudisco E (2016) Localized deformation in compression and folding of paperboard. Pack Technol Sci 29:397–414
33. Borodulina S, Kulachenko A, Tjahjanto DD (2015) Constitutive modeling of a paper fiber in cyclic loading applications. Comput Mater Sci 110:227–240
34. Borodulina S, Motamedian HR, Kulachenko A (2018) Effect of fiber and bond strength variations on the tensile stiffness and strength of fiber networks. Int J Solids Struct 154:19–32
35. Borodulina S, Wernersson ELG, Kulachenko A, Luengo Hendriks CL (2016) Extracting fiber and network connectivity data using microtomography images of paper. Nord Pulp Pap Res J 31:469–478
36. Bosco E, Peerlings RHJ, Geers MGD (2015) Predicting hygro-elastic properties of paper sheets based on an idealized model of the underlying fibrous network. Int J Solids Struct 56–57:43–52
37. Bosco E, Peerlings RHJ, Geers MGD (2015) Explaining irreversible hygroscopic strains in paper: a multi-scale modelling study on the role of fibre activation and micro-compressions. Mech Mater 91:76–94
38. Bosco E, Peerlings RHJ, Geers MGD (2017) A micro-mechanical modelling study of drying restraint effects on the hygro-mechanics of paper sheets. In: Transactions of the 16th fundamental research symposium, pp 627–649
39. Brandberg A, Kulachenko A (2017) The effect of geometry changes on the mechanical stiffness of fibre–fibre bonds. In: Transactions of the 16th fundamental research symposium, pp 683-719
40. Brandberg A, Kulachenko A (2019) New insights into compressive strength of paper board. In: Proceedings of the international paper physics conference, pp 134–139
41. Bronlund JE, Redding GP, Robertson TR (2014) Modelling steady-state moisture transport through corrugated fibreboard packaging. Pack Technol Sci 27:193–201
42. Bruhns OT (2019) History of plasticity. Encycl Contin Mech 6:1–61
43. Camanho PP, Davila CG, De Moura MF (2003) Numerical simulation of mixed-mode progressive delamination in composite materials. J Compos Mater 37:1415–1438
44. Câmpean T, Grad F, Grădinariu C, Patraşcu C, Gavrilescu M, Gavrilescu DA (2017) Eco-friendly corrugated board and sustainable package manufacturing. Environ Eng Manag J 16:705–714
45. Cerrone A, Wawrzynek P, Nonn A, Paulino GH, Ingraffea A (2014) Implementation and verification of the Park–Paulino–Roesler cohesive zone model in 3D. Eng Fract Mech 120:26–42
46. Charfeddine MA, Bloch JF, Boller E, Mangin P (2016) 3D synchrotron X-ray microtomography for paper structure characterization of z-structured paper by introducing micro nanofibrillated cellulose. Nordic Pulp Pap J 31:218–223
47. Charfeddine MA, Bloch JF, Mangin P (2019) Mercury porosimetry and X-ray microtomography for 3-dimensional characterization of multilayered paper: nanofibrillated cellulose, thermomechanical pulp, and a layered structure involving both. BioResources 14:2642–2650
48. Chen L, Zhou J, Tao J (2019) Study of the effectiveness of the RVEs for random short fiber reinforced elastomer composites. Fibers Polym 20:1467–1479
49. Chen N, Silberstein MN (2019) A micromechanics-based damage model for non-woven fiber networks. Int J Solids Struct 160:18–31
50. Cherkaev A, Ryvkin M (2019) Damage propagation in 2d beam lattices: 1. Uncertainty and assumptions. Arch Appl Mech 89:485–501
51. Cherkaev A, Ryvkin M (2019) Damage propagation in 2d beam lattices: 2. Design of an isotropic fault-tolerant lattice. Arch Appl Mech 89:503–519
52. Chinga-Carrasco G (2009) Exploring the multi-scale structure of printing paper—a review of modern technology. J Microsc 234:211–242
53. Chinga-Carrasco G (2011) Cellulose fibres, nanofibrils and microfibrils: the morphological sequence of MFC components from a plant physiology and fibre technology point of view. Nanoscale Res Lett 6:417
54. Choi DD, Lavrykov SA, Ramarao BV (2012) Delamination in the scoring and folding of paperboard. Tappi J 11:61–66
55. Coffin DW (2012) Creep and relaxation. Mechanics of paper products. Walter de Gruyter, Berlin, pp 111–134
56. Coffin DW (2015) Some observations towards improved predictive models for box compression strength. Tappi J 14:537–545
57. Coffin DW, Nygårds M (2017) Creasing and folding. In: Transactions of the 16th fundamental research symposium, pp 69–136
58. Confalonieri F, Perego U (2017) Cohesive modeling of mixed mode delamination in paperboard laminates. Euromech Colloquium 592:74–75
59. Confalonieri F, Perego U (2019) A new framework for the formulation and validation of cohesive mixed-mode delamination models. Int J Solids Struct 164:168–190
60. Cox HL (1952) The elasticity and strength of paper and other fibrous materials. Br J Appl Phys 3:72–79
61. Czechowski L, Bieńkowska M, Szewczyk W (2018) Paperboard tubes failure due to lateral compression-experimental and numerical study. Compos Struct 203:132–141
62. Czibula C, Ganser C, Seidlhofer T, Teichert C, Hirn U (2019) Transverse viscoelastic properties of pulp fibers investigated with an atomic force microscopy method. J Mater Sci 6:1–14
63. Deganutti CAS, Vieira O, Yamamoto CI (2018) Analysis of mechanical response during folding of creased and uncreased paperboard. Int J Adv Eng Res Sci 5:270–276
64. DeMaio A, Lowe R, Patterson T, Ragauskas A (2006) Direct observations of bonding influence on the tensile creep behavior of paper. Nord Pulp Pap Res J 21:297–302
65. Deogekar S, Picu RC (2018) On the strength of random fiber networks. J Mech Phys Solids 116:1–16
66. Dimitri R, Trullo M, De Lorenzis L, Zavarise G (2015) Coupled cohesive zone models for mixed-mode fracture: a comparative study. Eng Fract Mech 148:145–179
67. Dirrenberger J, Forest S, Jeulin D (2014) Towards gigantic RVE sizes for 3D stochastic fibrous networks. Int J Solids Struct 51:359–376
68. Domaneschi M, Perego U, Borgqvist E, Borsari R (2017) An industry-oriented strategy for the finite element simulation of paperboard creasing and folding. Pack Technol Sci 30:269–294
69. Dominic CA, Östlund S, Buffington J, Masoud MM (2015) Towards a conceptual sustainable packaging development model: a corrugated box case study. Pack Technol Sci 28:397–413
70. Drucker DC, Prager W (1952) Soil mechanics and plastic analysis or limit design. Q Appl Math 10:157–165

71. Ebner T, Hirn U, Fischer WJ, Schmied FJ, Schennach R, Ulz MH (2016) A proposed failure mechanism for pulp fiber–fiber joints. BioResources 11:9596–9610
72. Ekman A, Miettinen A, Tallinen T, Timonen J (2014) Contact formation in random networks of elongated objects. Phys Rev Lett 113:268001-1–268001-5
73. Ekman A, Miettinen A, Turpeinen T, Backfolk K, Timonen J (2012) The number of contacts in random fibre networks. Nord Pulp Pap Res J 27:270–276
74. El-Sayed S, Sridharan S (2001) Predicting and tracking interlaminar crack growth in composites using a cohesive layer model. Compos B Eng 32:545–553
75. Erkkilä AL, Leppänen T, Hämäläinen J, Tuovinen T (2015) Hygro-elasto-plastic model for planar orthotropic material. Int J Solids Struct 62:66–80
76. Fadiji T, Ambaw A, Coetzee CJ, Berry TM, Opara UL (2018) Application of finite element analysis to predict the mechanical strength of ventilated corrugated paperboard packaging for handling fresh produce. Biosyst Eng 174:260–281
77. Fadiji T, Coetzee CJ, Berry TM, Ambaw A, Opara UL (2018) The efficacy of finite element analysis (FEA) as a design tool for food packaging: a review. Biosyst Eng 174:20–40
78. Fadiji T, Coetzee CJ, Opara UL (2019) Analysis of the creep behaviour of ventilated corrugated paperboard packaging for handling fresh produce—an experimental study. Food Bioprod Process 117:126–137
79. Fellers C, Andersson C (2018) Evaluation of the stress–strain properties in the thickness direction—particularly for thin and strong papers. Nordic Pulp Pap Res J 27:287–294
80. Fellers C, Östlund S, Mäkelä P (2012) Evaluation of the Scott bond test method. Nord Pulp Pap Res J 27:231–236
81. Fischer WJ, Hirn U, Bauer W, Schennach R (2012) Testing of individual fiber–fiber joints under biaxial load and simultaneous analysis of deformation. Nord Pulp Pap Res J 27:237–244
82. Ganser C, Hirn U, Rohm S, Schennach R, Teichert C (2014) AFM nanoindentation of pulp fibers and thin cellulose films at varying relative humidity. Holzforschung 68(1):53–60
83. Giampieri A, Perego U, Borsari R (2011) A constitutive model for the mechanical response of the folding of creased paperboard. Int J Solids Struct 48:2275–2287
84. Girlanda O, Tjahjanto DD, Östlund S, Schmidt LE (2016) On the transient out-of-plane behaviour of high-density cellulose-based fibre mats. J Mater Sci 51:8131–8138
85. Golkhosh F, Targhagh M, Sharma Y, Martinez M, Tsai W, Courtois L, Eastwood D, Lee P, Phillion A (2016) 3D structure and strength characterization of northern bleached softwood kraft paper. Progr Pap Phys Semin
86. Goutianos S, Mao R, Peijs T (2018) Effect of inter-fibre bonding on the fracture of fibrous networks with strong interactions. Int J Solids Struct 136:271–278
87. Groche P, Huttel D (2016) Paperboard forming—specifics compared to sheet metal forming. BioResources 11:1855–1867
88. Groche P, Huttel D, Post PP, Schabel S (2012) Experimental and numerical investigation of the hydroforming behavior of paperboard. Prod Eng Res Devel 6:229–236
89. Gutkin R, Laffan ML, Pinho ST, Robinson P, Curtis PT (2011) Modelling the R-curve effect and its specimen-dependence. Int J Solids Struct 48:1767–1777
90. Hagman A, Nygårds M (2017) Thermographical analysis of paper during tensile testing and comparison to digital image correlation. Exp Mech 57:325–339
91. Hagman A, Nygårds M (2018) TShort compression testing of multi-ply paperboard, influence from shear strength. Nordic Pulp Pap Res J 31:123–134
92. Hagman A, Timmermann B, Nygårds M, Lundin A, Barbier C, Fredlund M, Östlund S (2017) Experimental and numerical verification of 3D forming. In: Transactions of the 16th fundamental research symposium, pp 3–26
93. Hallbäck N, Girlanda O, Tryding J (2006) Finite element analysis of ink-tack delamination of paperboard. Int J Solids Struct 43:899–912
94. Hallbäck N, Korin C, Barbier C, Nygårds M (2014) Finite element analysis of hot melt adhesive joints in carton board. Pack Technol Sci 27:701–712
95. Haslach HW (2000) The moisture and rate-dependent mechanical properties of paper: a review. Mech Time Depend Mater 4:169–210
96. Harrysson A, Ristinmaa M (2007) Description of evolving anisotropy at large strains. Mech Mater 39:267–282
97. Harrysson A, Ristinmaa M (2008) Large strain elasto-plastic model of paper and corrugated board. Int J Solids Struct 45:3334–3352
98. Hägglund R, Isaksson P (2008) On the coupling between macroscopic material degradation and interfiber bond fracture in an idealized fiber network. Int J Solids Struct 45:868–878
99. Hägglund R, Isaksson P (2015) Modeling deformation and damage of random fiber network (RFN) materials. Handb Damage Mech 8:1349–1368
100. Haj-Ali R, Choi J, Wei BS, Popil R, Schaepe M (2009) Refined nonlinear finite element models for corrugated fiberboards. Compos Struct 87:321–333
101. Hämäläinen P, Hallbäck N, Gåård A, Lestelius M (2017) On the determination of transverse shear properties of paper using the short span compression test. Mech Mater 107:22–30
102. Hill R (1948) A theory of the yielding and plastic flow of anisotropic metals. Proc R Soc Lond 193:281–297
103. Hirn U, Schennach R (2015) Comprehensive analysis of individual pulp fiber bonds quantifies the mechanisms of fiber bonding in paper. Sci Rep 5:1–9
104. Hirn U, Schennach R (2017) Fiber-fiber bon formation and failure: mechanisms and analytical techniques. In: Transactions of the 16th fundamental research symposium, pp 839–863
105. Hirn U, Schennach R, Ganser C, Magnusson M, Teichert C, Östlund S (2013) The area in molecular contact in fiber-fiber bonds. In: Transactions of the 15th fundamental research symposium, pp 8–13
106. Hossain S, Bergström P, Sarangi S, Uesaka T (2017) Computational design of fiber network by discrete element method. In: Transactions of the 16th fundamental research symposium, pp 651–668
107. Hossain S, Bergström P, Uesaka T (2019) Uniaxial compression of three-dimensional entangled fibre networks: impacts of contact interactions. Modell Simul Mater Sci Eng 27:015006
108. Höwer D, Lerch BA, Bednarcyk BA, Pineda EJ, Reese S, Simon JW (2018) Cohesive zone modeling for mode I facesheet to core delamination of sandwich panels accounting for fiber bridging. Compos Struct 183:568–581
109. Huang H, Hagman A, Nygårds M (2014) Quasi static analysis of creasing and folding for three paperboards. Mech Mater 69:11–34
110. Huang H, Nygårds M (2010) A simplified material model for finite element analysis of paperboard creasing. Nord Pulp Pap Res J 25:505–512
111. Huang H, Nygårds M (2011) Numerical and experimental investigation of paperboard folding. Nord Pulp Pap Res J 26:452–467
112. Huang H, Nygårds M (2012) Numerical investigation of paperboard forming. Nord Pulp Pap Res J 27:211–225
113. Huang X, Wang Q, Zhou W, Li J (2013) A simple fracture energy prediction method for fiber network based on its morphological features extracted by X-ray tomography. Mater Sci Eng A 585:297–303

114. Hussain S, Coffin DW, Todoroki C (2017) Investigating creep in corrugated packaging. Pack Technol Sci 30:757–770
115. Isaksson P, Gradin PA, Kulachenko A (2006) The onset and progression of damage in isotropic paper sheets. Int J Solids Struct 43:713–726
116. Isaksson P, Hägglund R (2007) Evolution of bond fractures in a randomly distributed fiber network. Int J Solids Struct 44:6135–6147
117. Isaksson P, Hägglund R (2009) Structural effects on deformation and fracture of random fiber networks and consequences on continuum models. Int J Solids Struct 46:2320–2329
118. Isaksson P, Hägglund R, Gradin PA (2004) Continuum damage mechanics applied to paper. Int J Solids Struct 41:4731–4755
119. Isaksson P, Gradin PA, Östlund S (2010) A simplified treatise of the Scott bond testing method. Exp Mech 50:745–751
120. Jajcinovic M, Fischer WJ, Hirn U, Bauer W (2016) Strength of individual hardwood fibres and fibre to fibre joints. Cellulose 23:2049–2060
121. Jajcinovic M, Fischer WJ, Matuner A, Bauer W, Hirn U (2016) Influence of relative humidity on the strength of hardwood and softwood pulp fibres and fibre to fibre joints. Cellulose 25:2681–2690
122. Jina W, Nagasawa S (2018) Finite element analysis of the folding process of creased white-coated paperboard using a combined fluffing resistance and shear yield glue model. J Adv Mech Des Syst Manuf 12:1–15
123. Jiang F, Weng J, Jia M, Yang Y, Zhang X (2018) Microstructural model in COMSOL packages with simulation to aging behavior of paper materials. Cellulose 25:1539–1553
124. Kappel L, Hirn U, Bauer W, Schennach R (2009) A novel method for the determination of bonded area of individual fiber–fiber bonds. Nord Pulp Pap Res J 24:199–205
125. Kappel L, Hirn U, Gilli E, Bauer W, Schennach R (2010) Revisiting polarized light microscopy for fiber–fiber bond area measurement—part I: theoretical fundamentals. Nord Pulp Pap Res J 25:62–70
126. Kappel L, Hirn U, Gilli E, Bauer W, Schennach R (2010) Revisiting polarized light microscopy for fiber–fiber bond area measurement—part II: proving the applicability. Nord Pulp Pap Res J 25:71–75
127. Karafillis AP, Boyce MC (1993) A general anisotropic yield criterion using bounds and a transformation weighting tensor. J Mech Phys Solids 41:1859–1882
128. Karakoç A, Hiltunen E, Paltakari J (2017) Geometrical and spatial effects on fiber network connectivity. Compos Struct 168:335–344
129. Karlsson J, Schill M, Tryding J (2016) `*MAT\_PAPER` and `*MAT\_COHESIVE\_PAPER`: two new models for paperboard materials. In: 14th International LS-DYNA users conference, pp 1.1–1.12
130. Ketoja JA, Paunonen S, Jetsu P, Pääkkönen E (2019) Compression strength mechanisms of low-density fibrous materials. Materials 12:384
131. Klingberg M, Boldizar A, Hofer K (2018) Mechanical properties of paperboard with a needled middle layer. Cellul Chem Technol 52:89–97
132. Kouko J, Jajcinovic M, Fischer W, Ketola A, Hirn U, Retulainen E (2019) Effect of mechanically induced micro deformations on extensibility and strength of individual softwood pulp fibers and sheets. Cellulose 26:1995–2012
133. Kouko J, Retulainen E (2015) The influence of strain rate and pulp properties on the stress–strain curve and relaxation rate of wet paper. Tappi J 14:515–524
134. Köstner V, Ressel JB, Sadlowsky B, Böröcz P (2017) Individual test rig for measuring the creep behaviour of corrugated board for packaging. Acta Technica Jaurinensis 10:148–156
135. Köstner V, Ressel JB, Sadlowsky B, Böröcz P (2018) Measuring the creep behaviour of corrugated board by cascade and individual test rig. J Appl Pack Res 10:46–61
136. Krasnoshlyk V, Rolland du Roscoat S, Dumont PJJ, Isaksson P (2018) Influence of the local mass density variation on the fracture behavior of fiber network materials. Int J Solids Struct 138:236–244
137. Kulachenko A, Uesaka T (2012) Direct simulations of fiber network deformation and failure. Mech Mater 51:1–14
138. Lahti J, Dauer M, Keller DS, Hirn U (2017) Linking paper structure to local distribution of deformation and damage. In: Transactions of the 16th fundamental research symposium, pp 669–682
139. Latifi SK, Saketi P, Kallio P (2014) Experimental evaluation of z-firectional fibre–fibre bond strength using microrobotics. In: International conference on manipulation, manufacturing and measurement on the nanoscale, pp 335–340
140. Lavrykov S, Lindström SB, Singh KM, Ramarao BV (2012) 3D network simulations of paper structure. Nord Pulp Pap Res J 27:256–263
141. Lee S, Yoon GH (2017) Moisture transport in paper passing through the fuser nip of a laser printer. Cellulose 24:3489–3501
142. Leppänen T, Erkkilä A-L, Kouko J, Laine V, Sorvari J (2017) A plasticity model for predicting the rheological behavior of paperboard. Int J Solids Struct 106–107:38–45
143. Leppänen T, Sorvari J, Erkkilä A-L, Hämäläinen J (2005) Mathematical modelling of moisture induced out-of-plane deformation of a paper sheet. Modell Simul Mater Sci Eng 13:841–850
144. Li Y, Reese S, Simon JW (2018) Modeling the fiber bridging effect in cracked wood and paperboard using a cohesive zone model. Eng Fract Mech 196:83–97
145. Li Y, Stier B, Bednarcyk BA, Reese S, Simon JW (2016) The effect of fiber misalignment on the homogenized properties of unidirectional fiber reinforced composites. Mech Mater 92:261–274
146. Li Y, Stapleton S, Reese S, Simon JW (2016) Anisotropic elastic-plastic deformation of paper: in-plane model. Int J Solids Struct 100–101:286–296
147. Li Y, Stapleton S, Reese S, Simon JW (2018) Anisotropic elastic-plastic deformation of paper: out-of-plane model. Int J Solids Struct 130–131:172–182
148. Li Y, Stapleton S, Reese S, Simon JW (2016) Experimental and numerical study of paperboard interface properties. Exp Mech 56:1477–1488
149. Li Y, Yu Z, Reese S, Simon JW (2018) Evaluation of the out-of-plane response of fiber networks with a representative volume element model. Tappi J 17:329–339
150. Li H, Zhang H, Zhang F, Li X, Legere S, Ni Y (2018) Determination of interfiber bonded area based on the confocal laser scanning microscopy technique. ACS Publ 57:6153–6160
151. Lindner M (2018) Factors affecting the hygroexpansion of paper. J Mater Sci 53:1–26
152. Linvill E, Östlund S (2014) The combined effects of moisture and temperature on the mechanical response of paper. Exp Mech 54:1329–1341
153. Linvill E, Östlund S (2016) Biaxial in-plane yield and failure of paperboard. Nord Pulp Pap Res J 31:659–667
154. Linvill E, Östlund S (2016) Parametric study of hydroforming of paper materials using the explicit finite element method with a moisture-dependent and temperature-dependent constitutive model. Pack Technol Sci 29:145–160
155. Linvill E, Wallmeier M, Östlund S (2017) A constitutive model for paperboard including wrinkle prediction and

post-wrinkle behavior applied to deep drawing. Int J Solids Struct 117:143–158
156. Lipponen P, Leppänen T, Kouko J, Hämäläinen J (2008) Elasto-plastic approach for paper cockling phenomenon: on the importance of moisture gradient. Int J Solids Struct 45:3596–3609
157. Liu JX, Chen ZT, Li KC (2010) A 2-D lattice model for simulating the failure of paper. Theoret Appl Fract Mech 54:1–10
158. Liu JX, Chen ZT, Wang H, Li KC (2011) Elasto-plastic analysis of influences of bond deformability on the mechanical behavior of fiber networks. Theoret Appl Fract Mech 55:131–139
159. Lorbach C, Fischer WJ, Gregorova A, Hirn U, Bauer W (2014) Pulp fiber bending stiffness in wet and dry state measured from moment of inertia and modulus of elasticity. BioResources 9:5511–5528
160. Lorbach C, Hirn U, Kritzinger J, Bauer W (2012) Automated 3D measurement of fiber cross section morphology in handsheets. Nord Pulp Pap Res J 27:264–269
161. Lu XZ, Teng JG, Ye LP, Jiang JJ (2005) Bond-slip models for FRP sheets/plates bonded to concrete. Eng Struct 27:920–937
162. Lübke J, Wettlaufer M, Kiziltoprak N, Drass M, Schneider J, Knaack U (2018) Honeycomb-paperboard glass composite beams. Ce/papers 2:57–69
163. Luong VD, Abbès B, Abbès F, Nolot JB, Erre D (2019) Experimental characterisation and finite element modelling of paperboard for the design of paperboard packaging. IOP Conf Ser Mater Sci Eng 540:012014
164. Ma YH, Zhu HX, Su B, Hu GK, Perks R (2018) The elasto-plastic behaviour of three-dimensional stochastic fibre networks with cross-linkers. J Mech Phys Solids 110:155–172
165. Magnusson MS (2016) Investigation of interfibre joint failure and how to tailor their properties for paper strength. Nord Pulp Pap Res J 31:109–122
166. Magnusson MS, Östlund S (2011) Inter-fibre bond strength and combined normal and shear loading. Progr Pap Phys Semin
167. Magnusson MS, Östlund S (2013) Numerical evaluation of interfibre joint strength measurements in terms of three-dimensional resultant forces and moments. Cellulose 20:1691–1710
168. Magnusson MS, Zhang X, Östlund S (2013) Experimental evaluation of the interfibre joint strength of papermaking fibres in terms of manufacturing parameters and in two different loading directions. Exp Mech 53:1621–1634
169. Magnusson MS, Fischer WJ, Östlund S, Hirn U (2013) Interfibre joint strength under peeling, shearing and tearing types of loading. In: Transactions of the 15th fundamental research symposium, pp 103–124
170. Mäkelä P, Östlund S (2003) Orthotropic elastic-plastic material model for paper materials. Int J Solids Struct 40:5599–5620
171. Mäkelä P, Östlund S (2012) Cohesive crack modelling of thin sheet material exhibiting anisotropy, plasticity and large-scale damage evolution. Eng Fract Mech 79:50–60
172. Mansour R, Kulachenko A, Chen W, Ollson M (2019) Stochastic constitutive model of isotropic thin fiber networks based on stochastic volume elements. Materials 12:538–565
173. Martoïa F, Orgéas L, Dumont PJJ, Bloch JF, Flin F, Viguié J (2017) Crumpled paper sheets: low-cost biobased cellular materials for structural applications. Mater Des 136:150–164
174. Marulier C, Dumont PJJ, Orgéas L, Caillerie D, Rolland du Roscoat S (2012) Towards 3D analysis of pulp fibre networks at the fibre and bond levels. Nord Pulp Pap Res J 27:245–255
175. Marulier C, Dumont PJJ, Orgéas L, Rolland du Roscoat S, Caillerie D (2015) 3D analysis of paper microstructures at the scale of fibres and bonds. Cellulose 22:1517–1539
176. McKee RC, Gander JW, Wachuta JR (1963) Compression strength formula for corrugated boxes. Paperboard Pack 48:149–159
177. Meherishi L, Narayana SA, Ranjani KS (2019) Sustainable packaging for supply chain management in the circular economy: a review. J Clean Prod 237:117582
178. Miehe C, Göktepe S, Lulei F (2004) A micro-macro approach to rubber-like materials—part I: the non-affine micro-sphere model of rubber elasticity. J Mech Phys Solids 52:2617–2660
179. Motamedian HR, Kulachenko A (2018) Rotational constraint between beams in 3-D space. Mech Sci 9:373–387
180. Motamedian HR, Kulachenko A (2019) Simulating the hygro-expansion of paper using a 3D beam network model and concurrent multiscale approach. Int J Solids Struct 161:23–41
181. Navaranjan N, Dickson A, Paltakari J, Ilmonen K (2013) Humidity effect on compressive deformation and failure of recycled and virgin layered corrugated paperboard structures. Compos B Eng 45:965–971
182. Nagasawa S (2017) Engineering estimation of time-dependent deformation characteristics as bending moment relaxation and released unfolding motion of creased paperboard. IOP Conf Ser Mater Sci Eng 175:012003
183. Nagasawa S, Kaneko S, Adachi D (2019) Effects of rotational velocity and hold time at folding posture on time-dependent release behavior of creased white-coated paperboard. J Adv Mech Des Syst Manuf 13(jamdsm0004):1–10
184. Neagu RC, Gamstedt EK (2007) Modelling of effects of ultra-structural morphology on the hygroelastic properties of wood fibres. J Mater Sci 42:10254–10274
185. Neale KW, Ebead UA, Baky HA, Elsayed WE, Godat A (2006) Analysis of the load-deformation behaviour and debonding for FRP-strengthened concrete structures. Adv Struct Eng 9:751–763
186. Negi V, Picu RC (2019) Mechanical behavior of cross-linked random fiber networks with inter-fiber adhesion. J Mech Phys Solids 122:418–434
187. Nygårds M (2008) Experimental techniques for characterization of elastic-plastic material properties in paperboard. Nord Pulp Pap Res J 23:432–437
188. Nygårds M (2009) Modelling the out-of-plane behaviour of paperboard. Nord Pulp Pap Res J 24:72–76
189. Nygårds M, Bhattacharya A, Krishnan SVR (2014) Optimizing shear strength profiles in paperboard fo better crease formation. Nord Pulp Pap Res J 29:510–520
190. Nygårds M, Fellers C, Östlung S (2007) Measuring out-of-plane shear properties of paperboard. J Pulp Pap Sci 33:105–109
191. Nygårds M, Fellers C, Östlung S (2009) Development of the notched shear test. In: 14th Fundamental research symposium, pp 14–18
192. Nygårds M, Hallbäck N, Just M, Tryding J (2005) A finite element model for simulations of creasing and folding of paperboard. In: Abaqus users' conference
193. Nygårds M, Just M, Tryding J (2009) Experimental and numerical studies of creasing of paperboard. Int J Solids Struct 46:2493–2505
194. Nygårds M, Malnory J (2010) Measuring the out-of-plane shear strength profiles in different paper qualities. Nord Pulp Pap Res J 25:366–371
195. Nygårds M, Sjökvist S, Marin G, Sundström J (2019) Simulation and experimental verification of a drop test and compression test of a gable top package. Pack Technol Sci 1–9
196. Ojha A, Sharma A, Sihag M, Ojha S (2015) Food packaging-materials and sustainability—a review. Agric Rev 36:241–245
197. Oria C, Ortiz A, Ferreño D, Carrascal I, Fernández I (2019) State-of-the-art review on the performance of cellulosic dielectric materials in power transformers: mechanical response and ageing. IEEE Trans Dielectr Electr Insul 26:939–954
198. Östlund S (2017) Three-dimensional deformation and damage mechanisms in forming of advanced structures in paper. In:

Transactions of the 16th fundamental research symposium, pp 1–106
199. Ottosen NS, Ristinmaa M (2005) The mechanics of constitutive modeling. Elsevier, Amsterdam
200. Park K, Choi H, Paulino GH (2016) Assessment of cohesive traction-separation relationships in ABAQUS: a comparative study. Mech Res Commun 78:71–78
201. Park K, Paulino GH, Roesler JR (2009) A unified potential-based cohesive model of mixed-mode fracture. J Mech Phys Solids 57:891–908
202. Park K, Paulino GH (2012) Computational implementation of the PPR potential-based cohesive model in Abaqus: educational perspective. Eng Fract Mech 93:239–262
203. Persson K (2000) Micromechanical modelling of wood and fibre properties. Department of Mechanics and Materials, Lund University, Lund
204. Persson J, Isaksson P (2014) A mechanical particle model for analyzing rapid deformations and fracture in 3D fiber materials with ability to handle length effects. Int J Solids Struct 51:2244–2251
205. Pfeiffer M, Kolling S (2019) A non-associative orthotropic plasticity model for paperboard under in-plane loading. Int J Solids Struct 166:112–123
206. Pfeiffer M, Kolling S, Stein P, Franke W (2018) A modified in-plane constitutive model for paperboard. LS-DYNA Forum 15:1–9
207. Rahman AA, Urbanik TJ, Mahamid M (2006) FE analysis of creep and hygroexpansion response of a corrugated fiberboard to a moisture flow: a transient nonlinear analysis. Wood Fiber Sci 38:268–277
208. Ramberg W, Osgood WR (1943) Description of stress–strain curves by three parameters. Technical note of the National Advisory Committee for Aeronautics, p 902
209. Rappel H, Beex LAA (2019) Estimating fibres' material parameter distributions from limited data with the help of Bayesian inference. Eur J Mech A Solids 75:169–196
210. Reese S, Raible T, Wriggers P (2001) Finite element modelling of orthotropic material behaviour in pneumatic membranes. Int J Solids Struct 38:9525–9544
211. Reichel S, Kaliske M (2015) Hygro-mechanically coupled modelling of creep in wooden structures, part I: mechanics. Int J Solids Struct 77:28–44
212. Reichel S, Kaliske M (2015) Hygro-mechanically coupled modelling of creep in wooden structures, part II: influence of moisture content. Int J Solids Struct 77:45–64
213. Retulainen E, Parkkonen J, Miettinen A (2016) X-ray nanotomography of fiber bonds. Progr Pap Phys Semin 162–168
214. Ring GJF, Kurki M, Nieminen T (2015) An elliptical pore model for the mechanical properties of paper. Tappi J 14:507–514
215. Robertsson K, Borgqvist E, Wallin M, Ristinmaa M, Tryding J, Giampieri A, Perego U (2018) Efficient and accurate simulation of the packaging forming process. Pack Technol Sci 31:557–566
216. Runesson L (2016) Numerical and experimental study of embossing of paperboard. Master Thesis at the Karlstads Universitet
217. Saketi P, Kallio P (2011) Microrobotic platform for making, manipulating and breaking individual paper fiber bonds. In: IEEE international symposium on assembly and manufacturing, pp 1–6
218. Saketi P, Latifi SK, Hirvonen J, Rajala S, Vehkaoja A, Salpavaara T, Lekkala J, Kallio P (2015) PVDF microforce sensor for the measurement of Z-directional strength in paper fiber bonds. Sens Actuat A 222:194–203
219. Schill M, Tryding J, Karlsson J (2015) Simulation of forming of paperboard packaging using LS-DYNA. In: 10th European LS-DYNA conference, pp 1–9
220. Schmied FJ, Teichert C, Kappel L, Hirn U, Bauer W, Schennach R (2013) What holds paper together: nanometre scale exploration of bonding between paper fibres. Sci Rep 3:1–6
221. Schneider M, Kabel M, Andrä H, Lenske A, Hauptmann M, Majschak J-P, Penter L, Hardtmann A, Ihlenfeldt S, Westersteiger R, Glatt E, Wiegmann A (2016) Thermal fiber orientation tensors for digital paper physics. Int J Solids Struct 100–101:234–244
222. Sellén C, Isaksson P (2014) A mechanical model for dimensional instability in moisture-sensitive fiber networks. J Compos Mater 48:277–289
223. Sharma Y, Phillion AB, Martinez DM (2015) Automated segmentation of wood fibres in micro-CT images of paper. J Microsc 260:400–410
224. Simon JW, Höwer D, Stier B, Reese S (2015) Meso-mechanically motivated modeling of layered fiber reinforced composites accounting for delamination. Compos Struct 122:477–487
225. Simon JW, Höwer D, Stier B, Reese S, Fish J (2017) A regularized orthotropic continuum damage model for layered composites: intralaminar damage progression and delamination. Comput Mech 60:445–463
226. Sliseris J, Andrä H, Kabel M, Dix B, Plinke B (2017) Virtual characterization of MDF fiber network. Eur J Wood Wood Prod 75:397–407
227. Sliseris J, Andrä H, Kabel M, Dix B, Plinke B, Wirjadi O, Frolovs G (2014) Numerical prediction of the stiffness and strength of medium density fiberboards. Mech Mater 79:73–84
228. Sørensen BF, Jacobsen TK (1998) Large-scale bridging in composites: R-curves and bridging laws. Compos A Appl Sci Manuf 29:1443–1451
229. Sorvari J, Leppänen T, Silvennoinen J (2018) The effect of the through-thickness moisture content gradient on the moisture accelerated creep of paperboard: hygro-viscoelastic modeling approach. Nord Pulp Pap Res J 33:122–132
230. Sozumert E, Farukh F, Sabuncuoglu B, Demirci E, Acar M, Pourdeyhimi B, Silberschmidt VV (2020) Deformation and damage of random fibrous networks. Int J Solids Struct 184:233–247
231. Spencer A (1984) Continuum theory of the mechanics of fiber-reinforced composites, vol 282. Springer, Berlin
232. Spring DW, Giraldo-Londono O, Paulino GH (2016) A study on the thermodynamic consistency of the Park–Paulino–Roesler (PPR) cohesive fracture model. Mech Res Commun 78:100–109
233. Staub S, Andrä H, Kabel M (2018) Fast FFT based solver for rate-dependent deformations of composites and nonwovens. Int J Solids Struct 154:33–42
234. Stenberg N, Fellers C (2002) Out-of-plane Poisson's ratios of paper and paperboard. Nord Pulp Pap Res J 17:387–394
235. Stenberg N, Fellers C, Östlund S (2001) Plasticity in the thickness direction of paperboard under combined shear and normal loading. Trans ASME 123:184–190
236. Stenberg N (2003) A model for the through-thickness elastic-plastic behaviour of paper. Int J Solids Struct 40:7483–7498
237. Strömbro J, Gudmundson P (2008) Mechano-sorptive creep under compressive loading—a micromechanical model. Int J Solids Struct 45:2420–2450
238. Strömbro J, Gudmundson P (2008) An anisotropic fibre-network model for mechano-sorptive creep in paper. Int J Solids Struct 45:5765–5787
239. Svendsen B (2001) On the modelling of anisotropic elastic and inelastic material behaviour at large deformation. Int J Solids Struct 38:9579–9599
240. Tjahjanto DD, Girlanda O, Östlund S (2015) Anisotropic viscoelastic-viscoplastic continuum model for high-density cellulose-based materials. J Mech Phys Solids 84:1–20
241. Torgnysdotter A, Kulachenko A, Gradin P (2007) Fiber/fiber crosses: finite element modeling and comparison with experiment. J Compos Mater 41:1603–1618

242. Torgnysdotter A, Kulachenko A, Gradin P (2007) The link between the fiber contact zone and the physical properties of paper: a way to control paper properties. J Compos Mater 41:1619–1633
243. Tryding J, Marin G, Nygårds M, Mäkelä P, Ferrari G (2017) Experimental and theoretical analysis of in-plane cohesive testing of paperboard. Int J Damage Mech 26:895–918
244. Tryding J, Ristinmaa M (2017) Normalization of cohesive laws for quasi-brittle materials. Eng Fract Mech 178:333–345
245. Turon A, Camanho PP, Costa J, Dávila CG (2006) A damage model for the simulation of delamination in advanced composites under variable-mode loading. Mech Mater 38:1072–1089
246. van der Sman CG, Bosco E, Peerlings RH (2016) A model for moisture-induced dimensional instability in printing paper. Nord Pulp Pap Res J 31:676–683
247. Viguié J, Latil P, Orgéas L, Dumont PJJ, Rolland du Roscoat S, Bloch J-F, Marulier C, Guiraud O (2013) Finding fibres and their contacts within 3D images of disordered fibrous media. Compos Sci Technol 89:202–210
248. Vishtal A, Retulainen E (2014) Boosting the extensibility potential of fibre networks: a review. BioResources 9(4):7933–7983
249. Wallmeier M, Hauptmann M, Majschak J-P (2016) The occurrence of rupture in deep-drawing of paperboard. BioResources 11:4688–4704
250. Wallmeier M, Linvill E, Hauptmann M, Majschak J-P, Östlund S (2015) Explicit FEM analysis of the deep drawing of paperboard. Mech Mater 89:202–215
251. Wernersson ELG, Borodulina S, Kulachenko A, Borgefors G (2014) Characterisations of fibre networks in paper using micro computed tomography images. Nord Pulp Pap Res J 29:468–475
252. Wilbrink DV, Beex LAA, Peerlings RHJ (2013) A discrete network model for bond failure and frictional sliding in fibrous materials. Int J Solids Struct 50:1354–1363
253. Xia QS, Boyce M, Parks DM (2002) A constitutive model for the anisotropic elastic-plastic deformation of paper and paperboard. Int J Solids Struct 39:4053–4071
254. Zaheer M, Awais M, Rautkari L, Sorvari J (2018) Finite element analysis of paperboard under compressional load. Proc Manuf 17:1162–1170
255. Zappa E, Liu R, Bolzon G, Shahmardani M (2017) High resolution non-contact measurement techniques for three-dimensional deformation processes of paperboard laminates. Mater Today Proc 4:5872–5876
256. Zapata PAM, Fransen M, ten Thije BJ, Saes L (2013) Coupled heat and moisture transport in paper with application to a warm print surface. Appl Math Model 37:7273–7286
257. Zechner J, Janko M, Kolednik O (2013) Determining the fracture resistance of thin sheet fiber composites—paper as a model material. Compos Sci Technol 74:43–51
258. Zechner J, Kolednik O (2013) Paper multilayer with a fracture toughness of steel. J Mater Sci 48:5180–5187